Int J Clin Exp Med 2016;9(9):17772-17781
www.ijcem.com /ISSN:1940-5901/IJCEM0019207

Original Article

Effects of atorvastatin on adventitial angiogenesis and sympathetic nerves in silicone collars around rabbit carotid artery models

Sen Liu, Ping Wang, Jianhua Zhou, Wenqing Zheng, Lixia Liu, Weiping Ju

Department of Cardiology, Second Ward, Shandong Weihai Central Hospital, Weihai 264400, China

Received November 5, 2015; Accepted February 10, 2016; Epub September 15, 2016; Published September 30, 2016

Abstract: The primary objective of this paper is to investigate the influence of atorvastatin on adventitial angiogenesis and sympathetic nerves in silicone collars placed around rabbit carotid artery models. Forty-five rabbits were randomly assigned to three groups: the normal group, model group, or atorvastatin group, Animals in the normal group were fed a typical diet, and animals in the model group and atorvastatin group were fed 1% high-cholesterol diet beginning the second day after the silicone collar was placed around their carotid arteries. Intervention lasted for four weeks, after which Masson staining was used to observe pathomorphological changes in the carotid arteries. VEGF and CD31 immumohistochemical staining evaluated the angiogenesis of the carotid arterial wall, and color-coded microsphere data demonstrated that atorvastatin successfully reduced blood flow volume in capillaries of the arterial wall. TH and NPY immunofluorescent staining indicated that atorvastatin decreased sympathetic nerve regeneration and NPY expression around adventitial vasa vasorum. To summarize, atorvastatin inhibits carotid adventitial angiogenesis by affecting sympathetic nerve regeneration in rabbits on high-cholesterol diets.

Keywords: Vasa vasorum, angiogenesis, sympathetic nerve, atherosclerosis

Introduction

Angiogenesis is a biological process in which new vessels are formed from old capillaries by sprouting or separating via multiple steps, such as endothelial cell migration and proliferation. The vasa vasorum, a microvessel network that originates mainly from arterial adventitia, provides oxygen and nutrient substances to the outer layer of the arterial wall. Angiogenesis is an important feature of arteriosclerosis (AS). Adventitial vasa vasorum neogenesis is a process activated during arteriosclerosis, and increase in vasa vasorum density is considered a response to arterial wall thickening as plaque formation occurs. Study has shown that this proliferative response happens before either endothelial dysfunction or formation of intima or plaque [1, 2]. Adventitial vasa vasorum is regarded as the channel through which inflammatory mediators or cells enter the vascular wall, and thus cause formation of plaque or contribute to the development of atherosclerotic diseases [3, 4]. Anti-angiogenesis treatment can effectively decrease vasa vasorum density, and discourage further accumulation of plaque [5, 6].

Nerves and vessels constitute a complicated branching network within many tissues in the body, and are closely correlated with each other in terms of anatomy and function [7]. Regarding vascular anatomy, specifically, the peripheral nervous system is a highly important participant in the angiogenesis process, as are complete endothelial cells. Histological studies have shown that at the border between arterial adventitia and tunica media exist a great number of norepinephrine and cholinergic fibers, which release various neurotransmitters including norepinephrine and acetylcholine, and promote angiogenesis [8, 9]. During embryonic development, peripheral nerves promote structural formation and arterial differentiation of vascular branches [10, 11]. NPY, a neurotransmitter released from sympathetic nerves to

control cardiac blood vessels, has the potential effect of facilitating angiogenesis. In-vitro experiments have proven that NPY can promote human endothelial cell adhesion, migration, proliferation, and capillary lumen formation [12, 13]. In rat models of hind limb ischemia, local application of NPY was shown to significantly increase the densities of positive vessels vWF and CD31, and contribute to angiogenesis of ischemic tissue [14]. Additionally, previous research has reported that neural regulation is likely involved in inducing maturity and stability of new micro vessels [15].

Statins, a hydroxymethylglutaryl coenzyme A reductase inhibitor (HMG-CoA reductase inhibitor), extensively applied in reducing cholesterol and stabilizing atheromatous plaque, they demonstrably reduce the morbidity and mortality of coronary atherosclerotic heart disease and cerebral ischemic stroke. Data published in recent years suggest that statins have multiple effects independent of their characteristic quality of blood lipid regulation [16]. The effects of statins on angiogenesis, for example, have been investigated by several research projects. Previous literature indicates that statins exert two-way effects on angiogenesis. Simvastatin is proven to promote angiogenesis in animals with normal blood cholesterol levels [17]. In rat models of hind limb ischemia, atorvastatin strongly induced the expression of pro-angiogenesis cell factors, and increased the quantity of circulating endothelial cells [18]. Research has also reported that atorvastatin can suppress neogenesis of vasa vasorum and postpone the formation of plaque in apoE-/- mice [19]. Experimentation has demonstrated that statins play a role in inhibiting the migration and proliferation functions of in-vitro cultured endothelial cells, as well [20]. Further, statins seem to have dose-dependent effects on angiogenesis; low-dose statins promote cell proliferation and migration, while high-concentration statins suppress angiogenesis [21, 22]. The specific mechanism at work in the anti-angiogenesis effect of statins is yet unclear; however, sympathetic nerve regulation is very likely involved in the angiogenesis process. To this effect, this study investigates the influence of atorvastatin treatment on adventitial vasa vasorum and sympathetic nerves at early stages of atherosclerosis.

Materials and methods

Experimental animals

Normal, healthy, New Zealand white rabbits, 3-4 months old, male, with an average weight of 2.0 ± 0.2 Kg, were purchased from Beijing Fuhao Laboratory Animal Breeding Center (license no. SCXK [Beijing] 2010-0010).

Model establishment, grouping, and medication

Silicone collars, placed around the right common carotid artery, were established according to similar experiments on rat models [23]. 3% pentobarbital sodium (1 ml/Kg) was injected via ear vein to anesthetize the rabbits. After anesthesia and fur removal, the rabbit was fixed in a supine position on the operating table. Routine disinfection and draping were performed. The skin was incised under the thyroid cartilage and along the cervical midline, and each layer was separated by blunt dissection to expose the right common carotid artery sheath. 3-4 cm of carotid artery was separated with caution. A medical silicone tube 20 mm in length, 1.7 mm in internal diameter, and 3.2 mm in external diameter was cut longitudinally, then placed around the right common carotid artery of each New Zealand rabbit. Irrigation was performed with normal saline, the incision was sutured, and an intravenous drip of penicillin sodium was performed locally. After operation, local administration of penicillin sodium (800000 U/d, qd) was given for three consecutive days to prevent infection.

The 45 rabbits were fed adaptively for one week, then subject to carotid arterial tube placement and randomly assigned to the normal, model and atorvastatin group. There were 3 groups, each containing 15 rabbits. The normal group was supplied with typical feedstuffs. The model group and atorvastatin group were fed a high-lipid feedstuff, comprised of 1% cholesterol, 5% lard oil, 7.5% yolk powder, and 86.5% basal feed, produced by Yantai University Animal Center. Each rabbit was given 120 g of food twice per day.

In accordance with doses stipulated by this research group under the National 973 Program, rabbits in the atorvastatin group were given 2.50 mg/(Kg·d) of atorvastatin by gavage.

Intragastric administration was initiated the second day after the silicone tube was placed around the carotid artery. The experiment lasted four weeks.

Specimen collection

Specimen collection for each group was performed at the end of the four-week experimental period. Before sampling, the animals were subject to fasting for 12 hours. All animals were then euthanized with 3% pentobarbital sodium (1 ml/Kg). After the right common carotid artery was removed and washed by icy normal saline, the attached connective tissues were cautiously stripped. One segment of the sample was fixed in a 10% neutral formaldehyde solution for fabrication of paraffin sections, which were then used in Masson staining, immunohistochemical staining, and immunofluorescence experiments. The whole process was completed rapidly with an aseptic technique. In addition, nine rabbits were randomly selected from the three groups (three per group) for use in color-coded microsphere tests to determine blood flow volume within the micro vessels of the right carotid artery.

Masson staining

Samples successively underwent dewaxing, water scrubbing, Weigert's iron hematoxylin staining for 5-10 minutes, 1% hydrochloric acid alcohol differentiation, Xylidine Ponceau 2R staining for 5-10 minutes, treatment by 1% phosphomolybdic acid aqueous solution for 5 minutes, aniline blue counterstaining for 5 minutes, treatment by 1% glacial acetic acid for 1 minute, 95% alcohol dehydration, anhydrous alcohol dehydration, dimethylbenzene transparency, and neutral balsam mounting. Results showed that collagenous fibers were green, smooth muscle cells of the vascular wall were red, and cell nuclei were blue-brown.

Immunohistochemistry

EnVision immunohistochemistry was used to detect the localization and expression of VEGF and CD31 in carotid arterial tissues. After dewaxing of the paraffin section, each 5 μm-thick carotid arterial specimen was placed in a 3% H_2O_2 solution to block endogenous peroxidase. Primary antibody solution, made by diluting 5% BSA to scale (CD31 1:200 Abcam UK; VEGF 1:200 Abcam UK) covered the specimen tissue, which was incubated at 4°C overnight. HRP-labeled secondary antibody solution was added to cover the tissue. Color developing by DAB was performed. Cell nucleus counterstaining was conducted using Harris hematoxylin. The sections were dehydrated, made transparent, mounted, and observed under an optical microscope.

VEGF-positive staining results showed brown-yellow granules located in the cytoplasm. Results were judged according to the quantity of positive cells and position of positive signals. By referring to previous studies [24], the semi-quantitative integral method was utilized. Scores were gathered in accordance with positive cell rate and positive cell coloration intensity. CD31-positive coloring was located in the cytomembrane or cytoplasm. The method proposed by Weidner et al [25] was adopted to conduct quantitative analysis of CD31-labeled microvascular density (MVD), where first, the entire section was observed under 40 × light microscope to identify MVD "hotspot" areas. Next, 5 high-power fields were counted randomly under 400 × light microscope, and the average was considered the MVD of the specimen.

Immunofluorescence

Each paraffin section was subject to dewaxing and water scrubbing. After antigen retrieval, primary antibody fabricated by diluting 5% BSA to scale (TH 1:100 Abcam UK; NPY 1:200 Abcam UK) was added to cover the tissue. The sections were placed in a wet box and incubated at 4°C overnight. The slides were placed in PBS (pH7.4), then agitated and washed for 5 minutes on a color-drop table three separate times. Secondary antibody, corresponding to the primary antibody, was added to cover the tissue samples, which were then incubated in dark, room temperature conditions for 60 minutes. The slides were again placed in PBS (pH7.4) agitated, and washed on a color-drop table three times, for 5 minutes each time. Cell nucleus counterstaining by DAPI was then performed after the sections were slightly spin-dried. The sections were then incubated at room temperature in the dark for 10 minutes. After another slight spin-dry, the sections were

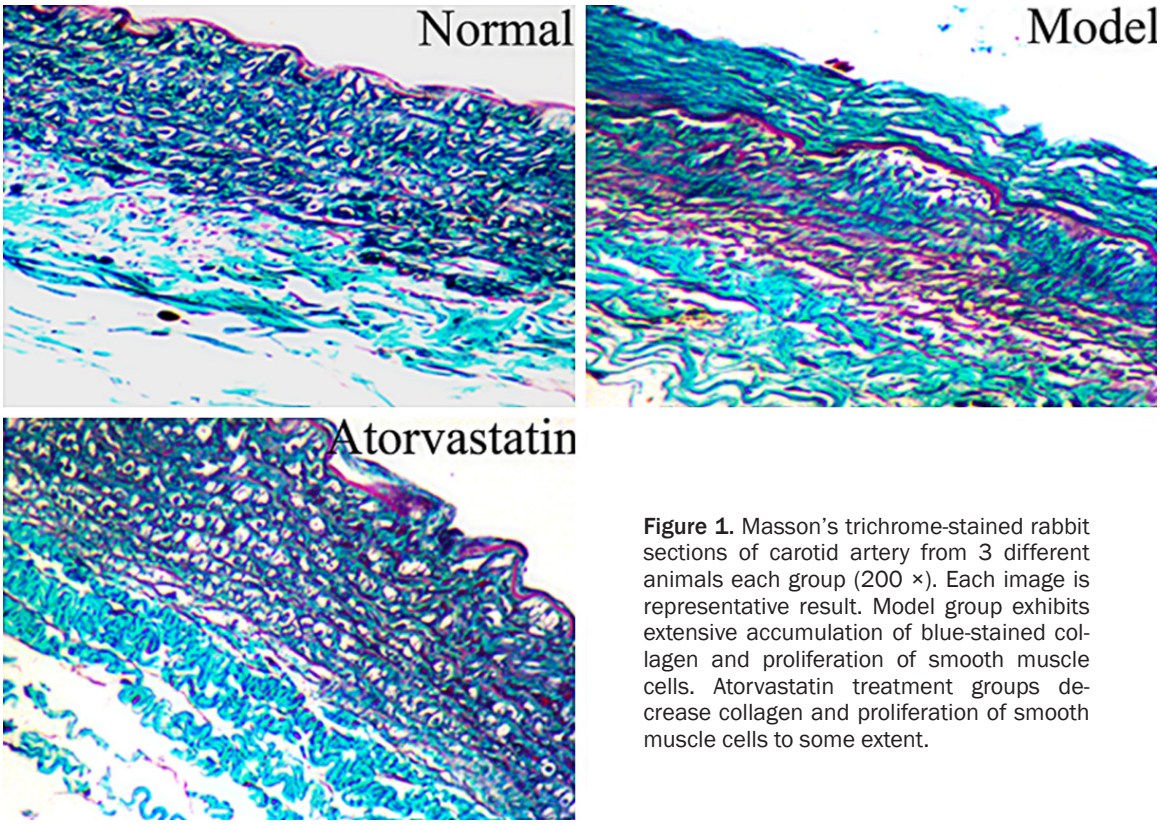

Figure 1. Masson's trichrome-stained rabbit sections of carotid artery from 3 different animals each group (200 ×). Each image is representative result. Model group exhibits extensive accumulation of blue-stained collagen and proliferation of smooth muscle cells. Atorvastatin treatment groups decrease collagen and proliferation of smooth muscle cells to some extent.

mounted with anti-fade fluorescence mounting medium and observed under IX71 inversed fluorescent microscope to acquire image data.

Blood flow measurement

DYE-TRAK color-code microspheres (Triton Technology, Inc., USA) were used to determine the blood flow of the carotid-arterial-wall vasa vasorum. The animals were anesthetized, fixed, and given femoral artery intubation. The second, third and fourth ribs were then removed to expose the heart. A 0.3 ml suspension containing 2.1×10^5 yellow microspheres (with maximum absorbance wavelength of 448 nm), and 0.2 ml of 0.05% Tween mixture was directly injected into the left cardiac ventricle by syringe in a 10 second interval. Blood and tissue specimens were retained. 5 seconds after microsphere injection, constant-velocity femoral arterial blood collection was performed for one minute. The right common carotid artery was removed immediately after femoral arterial blood collection. Blood and tissue samples were separately placed in 15 ml or 50 ml polypropylene centrifuge tubes, weighed in advance. After re-weighing, weights of blood sample and tissues were calculated. 100 μl suspension with a concentration of 1.0×10^5 blue microspheres/ml was added to each centrifuge tube as an internal control. By utilizing strong base dissolution, the sedimentation method was employed for recycling microspheres incarcerated in carotid arterial tissue. 200 μl of acidulated ethyl ethoxyacetate was used to extract dyestuff on the microsphere surface. An ultraviolet-visible spectrophotometer was used to detect absorbance values for calculating microvascular blood flow volume of each organ or tissue. The obtained experimental data were input into software supplied by Triton Technology, and microvascular blood flow volumes of each group were calculated (unit: μl/min·g).

Statistical analysis

Continuous data are expressed as mean ± S.D. and analyzed using SPSS 19.0 statistical software (SPSS Inc., Chicago, IL, USA). Differences between groups were analyzed by one-way analyses of variance (ANOVA) followed by Dunnett's test. A probability level of $P < 0.05$ was considered statistically significant.

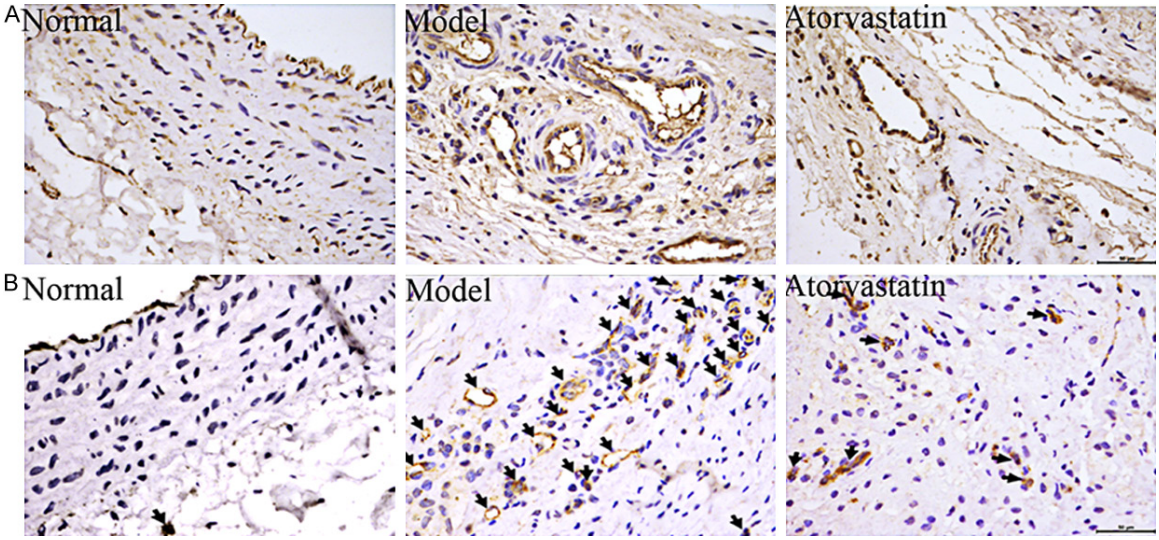

Figure 2. Immunohistology for vascular endothelial growth factor A (VEGF) and CD31 in cross sections of rabbit carotid arteries (400 ×). A. VEGF positive staining is localized predominantly in the adventitia. B. Microvessels were stained with CD31 antibody (400 ×). Arrows indicate CD31 positive vessels. Staining for vascular CD31: positive staining is localized to the adventitia. Atorvastatin inhibits adventia VEGF expression and the number of CD31 positive vessels in adventia in the rabbit carotid artery.

Table 1. Comparisons of the microvessel density and microvascular blood flow volume, VEGF+ expression in each group (n = 3, X ± S)

Group	MVD (n/mm^2)	VEGF+ (%)	MBF ($\mu l/min \cdot g$)
Normal	1.20 ± 0.35	0.09 ± 0.05	19.13 ± 2.91
Model	12.47 ± 0.81$^{\#}$	0.41 ± 0.07$^{\#}$	50.88 ± 8.46$^{\#}$
TXL-L	11.51 ± 0.87	0.38 ± 0.12	44.73 ± 4.42
TXL-M	2.73 ± 0.42**	0.20 ± 0.04**	35.66 ± 7.06**
TXL-H	1.93 ± 0.42$^{**,\blacktriangle}$	0.14 ± 0.01**	22.88 ± 4.82$^{**,\blacktriangle\blacktriangle}$
Atorvastatin	3.67 ± 1.21**	0.26 ± 0.04*	42.27 ± 5.69*
LY294002	2.67 ± 1.60**	0.21 ± 0.08**	30.30 ± 5.26$^{**,\blacktriangle}$
PD98058	2.80 ± 0.53**	0.23 ± 0.09*	36.36 ± 8.21**

Note: *vs.* Normal group: $^{\#}P < 0.01$; *vs.* Model group: $^{*}P < 0.05$, $^{**}P < 0.01$; *vs.* Atorvastatin group: $^{\blacktriangle}P < 0.05$, $^{\blacktriangle\blacktriangle}P < 0.01$.

Results

Masson staining of carotid artery

As illustrated in **Figure 1**, smooth muscle cells were dyed red, and collagenous fibers were blue. Carotid arterial tissues of the normal group showed clear structures in each layer, smooth intima, and regularly-arranged smooth muscle cells of tunica media. The model group presented significant thickening of vascular intima, migration of smooth muscle cells, massive deposition of collagenous fibers, and increased, disorderly-arranged smooth muscle cells of tunica media. The atorvastatin group had decreased intimal hyperplasia, mild collagenous fiber accumulation, and slightly increased, orderly-arranged tunica-media smooth muscle cells, with no migration of smooth muscle cell observed.

Angiogenesis of carotid arterial wall

Angiogenesis of the carotid arterial wall was granular, and primarily existent in the cytoplasm and extracellular matrix. A small amount of VEGF-positive expression was seen in intima, tunica media, and adventitia of the carotid arterial tissues of the normal group. In the model group, VEGF-positive expression significantly increased in each vessel layer, and positive expression was found in adventitial microvascular endothelial cells and their surroundings, as well as some adventitial fibroblasts. The atorvastatin group presented a certain degree of decline of VEGF-positive expression. Comparison between PBS-replaced VEGF monoclonal antibodies showed a negative result. VEGF-positive expression rate was used to identify VEGF-positive expression in adventitial tissue. The VEGF-positive expression rate of the model group was remarkably higher than the normal group, (statistical sig-

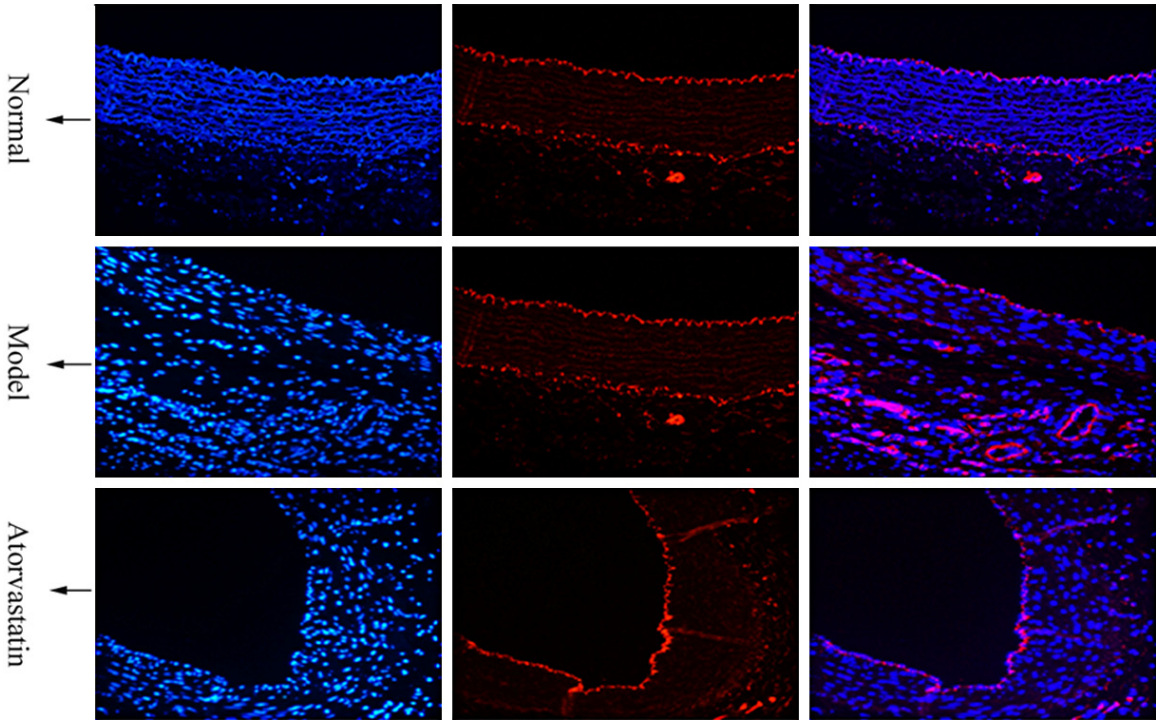

Figure 3. Expression of TH in the carotid artery is demonstrated by immunofluorescence (200 ×). Immunofluorescent staining for TH (red). The photographs are representative of 3 independent experiments.

nificance was $P < 0.01$). Compared to the model group, intervention by atorvastatin contributed to an obvious decrease in VEGF-positive expression rate ($P < 0.05$) (**Figure 2A**; **Table 1**).

In the carotid arteries of the normal group, a small number of CD31-labeled micro vessels were seen in the vascular adventitia. In the model group, the quantity of vascular-adventitial microvessels significantly increased, and no CD31-labeled microvessels were seen in the tunica media. In the atorvastatin group, the quantity of microvessels in adventitia declined considerably. Quantitative analysis of arterial-wall microvascular densities indicated that the MVD-positive labeling index of the model group was much higher than the normal group, and that the atorvastatin group showed a statistically significant ($P < 0.01$) reduction in MVD-positive labeling index compared to the model group (**Figure 2B**; **Table 1**).

Changes in microvascular blood flow of carotid arterial wall

Color-coded microsphere technology is a method which measures microvascular blood flow volume to a highly precise degree. In this study, DYE-TRAK color-coded microsphere technology was used to detect changes in microvascular blood flow of the carotid arterial wall samples. Carotid arterial microvascular blood flow volume of the model group was substantially higher than the normal group. Compared to the model group, the atorvastatin group showed an obvious decrease in microvascular blood flow (**Table 1**).

Immunofluorescence results

Tyrosine hydroxylase (TH) is a synthetase of endogenous catecholamine and a specific marker of sympathetic nerves. To determine the distribution of sympathetic nerves, this study employed immunofluorescence to observe tyrosine-hydroxylase (TH) expression. In the normal group, TH positive-labeled sympathetic nerves were distributed in endarterium and the tunica-media-adventitia border area. In the model group, sympathetic nerves distributed in the endarterium and tunica-media-adventitia border area decreased, but sympathetic nerve regeneration was found near the adventitial vasa vasorum. In the atorvastatin group, sympathetic nerve regeneration surrounding adventitial vasa vasorum was significantly reduced (**Figure 3**).

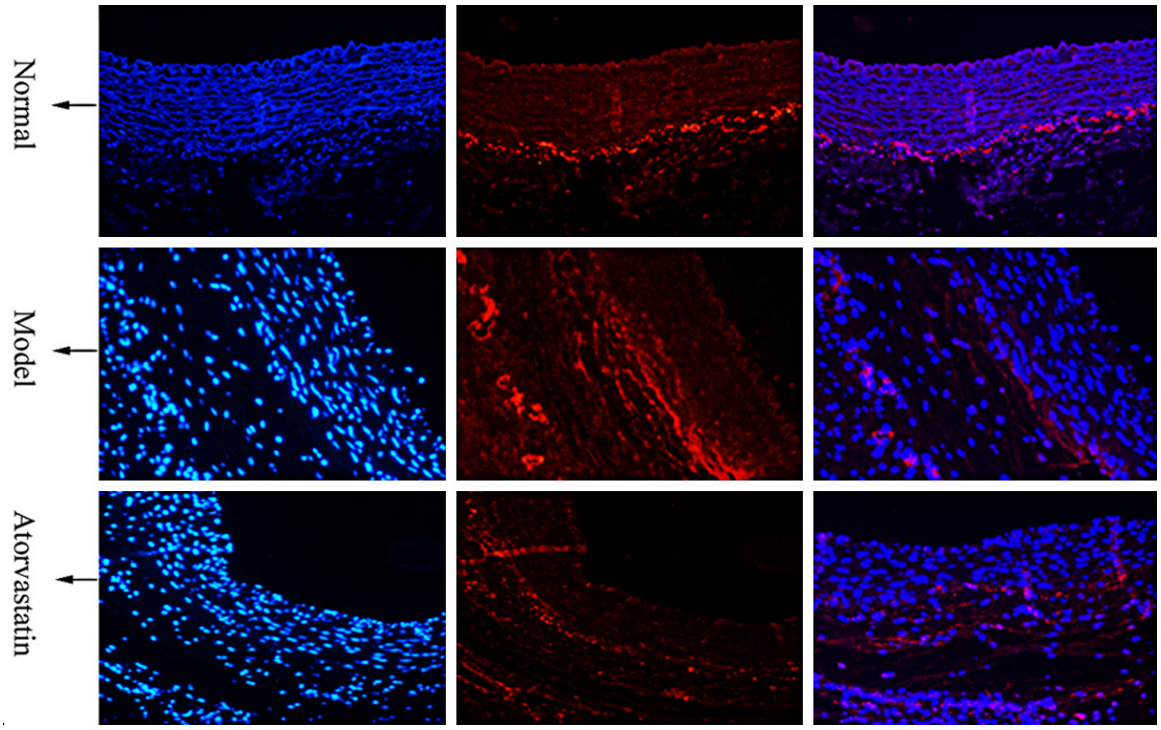

Figure 4. Expression of NPY in the carotid artery is demonstrated by immunofluorescence (200 ×). Immunofluorescent staining for NPY (red). The photographs are representative of 3 independent experiments.

Immunofluorescence demonstrated NPY-positive signals were primarily expressed in tunica-media-adventitia areas. In the model group, NPY-positive expression was strong around the vasa vasorum, but decreased at the tunica-media-adventitia border area. In the atorvastatin group, NPY-positive expression surrounding the adventitial vasa vasorum was markedly reduced (**Figure 4**).

Discussion

This study evaluated the effects of atorvastatin administration using silicone collars placed around the carotid arteries of rabbits with high blood cholesterol levels. Atorvastatin was proven to decrease adventitial VEGF-positive expression to a certain extent, and to inhibit adventitial angiogenesis, likely related to its roles in suppressing sympathetic nerve regeneration near adventitial microvessels and reducing NPY expression. Sympathetic nerves promote adventitial angiogenesis, and are indirectly involved in neointima formation by influencing pathological changes of vasa vasorum angiogenesis.

Neointima formation and intimal hyperplasia, both important pathological markers of atherosclerosis andrestenosis, are related to the adventitial vasa vasorum. Adventitial angiogenesis is considered to cause plaque instability and promote the formation of neointima. Experimental data suggests long-term application of angiogenesis inhibitors can suppress lesions and progress of atherosclerosis [26]. Additional research suggests a relationship between the degree of angiogenesis and the size of plaque deposits [27]. Angiogenesis is a result of the interaction between pro-angiogenesis factors and anti-angiogenesis factors. VEGF is the main regulatory factor of the angiogenesis process. In a previous study, VEGF-treated, cholesterol-fed mice were doubly deficient in apolipoprotein E/apolipoprotein B100, and clearly showed reinforced development of plaque [28]. In this study, atorvastatin down-regulated adventitial VEGF expression and inhibited adventitial angiogenesis. As a compensatory mechanism, angiogenesis re-allocates the blood flow volume of arterial-wall microvessels. This research used color-coded microspheres to detect changes in the blood flow volume of carotid-arterial-wall microvessels, and results showed that adventitial angiogenesis increases vasa vasorum blood flow volume while atorvastatin lowers arterial-wall mic-

rovascular blood flow volume. Decrease in microvascular blood flow may reduce neointimal hyperplasia. The significance of vasa vasorum neogenesis in neointimal formation has been proven in previous research [29].

It appears that sympathetic nerve regeneration stimulates adventitial angiogenesis to some degree. In this study, TH immunofluorescence testing revealed sympathetic nerve distribution around the vasa vasorum, indicating a relationship between sympathetic nerves and adventitial angiogenesis. In the normal group, sympathetic nerves were distributed in the endarterium and tunica-media-adventitia border area. In the model group, sympathetic nerves distributed at endarterium and tunica-media-adventitia border area decreased, but sympathetic nerve regeneration was found around the adventitial vasa vasorum. To this effect, it is speculated that highly differentiated and discrete sympathetic nerve density and function exist in the adventitial area. This can likely be attributed to the ischemic and anoxic environment of the tunica-media-adventitia border area restricting nerve growth, while the peri-vasa-vasorum environment stimulates sympathetic nerve regeneration. The inhibitory effect of atorvastatin on peri-vasa-vasorum sympathetic nerve regeneration may be one of the mechanisms at work which suppress adventitial angiogenesis.

According to experiment results detailed above, the microvascular blood flow volume of the arterial wall increases at the angiogenesis stage, and atorvastatin reduces the blood flow of the vasa vasorum. High-level sympathetic innervation around new vasa vasorum should have caused decrease in microvascular blood flow of the arterial wall, but in actuality, demonstrate the opposite effect, likely caused by the reduced sensitivity of to vasoconstrictive substances, but relatively increased sensitivity to vasodilative media. Previous research supports this speculation [30]. NPY, a type of neurotransmitter secreted by sympathetic nerves, stimulates angiogenesis primarily by activating Y2 acceptors, as demonstrated by previous research [31]. In-vitro experiments have proven that NPY stimulates activation, proliferation, and migration of endothelial cells, plus the formation of lumen. An experiment that embedded rat aortic rings in collagen proved that NPY stimulates the growth of vascular buds. The growth process was interrupted in eNOS gene knockout mice, indicating that NPY-mediated angiogenesis is achieved via eNOS [32]. NPY also induces expression of other growth factors, such as basic fibroblast growth factors (bFGF) and vascular endothelial growth factors (VEGF), which are downstream media of NPY-induced effects. Atorvastatin effectively decreases both sympathetic nerve regeneration and activity, and peri-microvessel NPY expression. This process is an important factor of reduced adventitial angiogenesis after atorvastatin treatment.

To conclude, this study is the first to prove specific inhibitory effects of atorvastatin on adventitial angiogenesis and sympathetic nerve regeneration through the use of carotid arterial silicone tubes and high-cholesterol diet testing on rabbits. The novel mechanism introduced here is the regeneration of adventitial sympathetic nerves inducing pathological, adventitial angiogenesis. This finding provides invaluable information for further research and development of atherosclerotic disease treatments.

Acknowledgements

This research received no specific grant from any funding agency in the public, commercial, or not-for-profit sectors.

Disclosure of conflict of interest

None.

Address correspondence to: Dr. Weiping Ju, Department of Cardiology, Second Ward, Shandong Weihai Central Hospital, Weihai 264400, China. Fax: +86-631-8801262; E-mail: jwpwendeng@126.com

References

[1] Fleiner M, Kummer M, Mirlacher M, Sauter G, Cathomas G, Krapf R, Biedermann BC. Arterial neovascularization and inflammation in vulnerable patients early and late signs of symptomatic atherosclerosis. Circulation 2004; 110: 2843-2850.

[2] Herrmann J, Lerman LO, Rodriguez-Porcel M, Holmes DR, Richardson DM, Ritman EL, Lerman A. Coronary vasa vasorum neovascularization precedes epicardial endothelial dysfunction in experimental hypercholesterolemia. Cardiovasc Res 2001; 51: 762-766.

[3] de Boer OJ, van der Wal AC, Teeling P, Becker AE. Leucocyte recruitment in rupture prone regions of lipid-rich plaques: a prominent role for neovascularization? Cardiovasc Res 1999; 41: 443-449.
[4] Kaartinen M, Penttilä A, Kovanen PT. Accumulation of activated mast cells in the shoulder region of human coronary atheroma, the predilection site of atheromatous rupture. Circulation 1994; 90: 1669-1678.
[5] Drinane M, Mollmark J, Zagorchev L, Moodie K, Sun B, Hall A, Shipman S, Morganelli P, Simons M, Mulligan-Kehoe MJ. The antiangiogenic activity of rPAI-123 inhibits vasa vasorum and growth of atherosclerotic plaque. Circ Res 2009; 104: 337-345.
[6] Moulton KS, Vakili K, Zurakowski D, Soliman M, Butterfield C, Sylvin E, Lo KM, Gillies S, Javaherian K, Folkman J. Inhibition of plaque neovascularization reduces macrophage accumulation and progression of advanced atherosclerosis. Proc Natl Acad Sci U S A 2003; 100: 4736-4741.
[7] Hao L, Zou Z, Tian H, Zhang Y, Song C, Zhou H, Liu L. Novel roles of perivascular nerves on neovascularization. Neurol Sci 2015; 36: 353-60.
[8] Chakroborty D, Sarkar C, Basu B, Dasgupta PS, Basu S. Catecholamines regulate tumor angiogenesis. Cancer Res 2009; 69: 3727-3730.
[9] Cooke JP, Ghebremariam YT. Endothelial nicotinic acetylcholine receptors and angiogenesis. Trends Cardiovasc Med 2008; 18: 247-253.
[10] Mukouyama YS, Shin D, Britsch S, Taniguchi M, Anderson DJ. Sensory nerves determine the pattern of arterial differentiation and blood vessel branching in the skin. Cell 2002; 109: 693-705.
[11] Mukouyama YS, Gerber HP, Ferrara N, Gu C, Anderson DJ. Peripheral nerve-derived VEGF promotes arterial differentiation via neuropilin 1-mediated positive feedback. Development 2005; 132: 941-952.
[12] Zukowska-Grojec Z, Karwatowska-Prokopczuk E, Rose W, Rone J, Movafagh S, Ji H, Yeh Y, Chen WT, Kleinman HK, Grouzmann E, Grant DS. Neuropeptide Ya novel angiogenic factor from the sympathetic nerves and endothelium. Circ Res 1998; 83: 187-195.
[13] Movafagh S, Hobson JP, Spiegel S, Kleinman HK, Zukowska Z. Neuropeptide Y induces migration, proliferation, and tube formation of endothelial cells bimodally via Y1, Y2, and Y5 receptors. FASEB J 2006; 20: 1924-1926.
[14] Lee EW, Michalkiewicz M, Kitlinska J, Kalezic I, Switalska H, Yoo P, Sangkharat A, Ji H, Li L, Michalkiewicz T, Ljubisavljevic M, Johansson H, Grant DS, Zukowska Z. Neuropeptide Y induces ischemic angiogenesis and restores function of ischemic skeletal muscles. J Clin Invest 2003; 111: 1853-1862.
[15] Asanome A, Kawabe JI, Matsuki M, Kabara M, Hira Y, Bochimoto H, Yamauchi A, Aonuma T, Takehara N, Watanabe T, Hasebe N. Nerve growth factor stimulates regeneration of perivascular nerve, and induces the maturation of microvessels around the injured artery. Biochem Biophys Res Commun 2014; 443: 150-155.
[16] Gotto AM, Whitney E, Stein EA, Shapiro DR, Clearfield M, Weis S, Jou JY, Langendörfer A, Beere PA, Watson DJ, Downs JR, de Cani JS. Relation between baseline and on-treatment lipid parameters and first acute major coronary events in the Air Force/Texas Coronary Atherosclerosis Prevention Study (AFCAPS/TexCAPS). Circulation 2000; 101: 477-484.
[17] Kureishi Y, Luo Z, Shiojima I, Bialik A, Fulton D, Lefer DJ, Sessa WC, Walsh K. The HMG-CoA reductase inhibitor simvastatin activates the protein kinase Akt and promotes angiogenesis in normocholesterolemic animals. Nat Med 2000; 6: 1004-1010.
[18] Matsumura M, Fukuda N, Kobayashi N, Umezawa H, Takasaka A, Matsumoto T, Yao EH, Ueno T, Negishi N. Effects of atorvastatin on angiogenesis in hindlimb ischemia and endothelial progenitor cell formation in rats. J Atheroscler Throm 2009; 16: 319-326.
[19] Bot I, Jukema JW, Lankhuizen IM, van Berkel TJ, Biessen EA. Atorvastatin inhibits plaque development and adventitial neovascularization in ApoE deficient mice independent of plasma cholesterol levels. Atherosclerosis 2011; 214: 295-300.
[20] Vincent Lc, Chen W, Hong L, Mirshahi F, Mishal Z, Mirshahi-Khorassani T, Vannier JP, Soria J, Soria C. Inhibition of endothelial cell migration by cerivastatin, an HMG-CoA reductase inhibitor: contribution to its anti-angiogenic effect. FEBS Lett 2001; 495: 159-166.
[21] Weis M, Heeschen C, Glassford AJ, Cooke JP. Statins have biphasic effects on angiogenesis. Circulation 2002; 105: 739-745.
[22] Dulak J, Loboda A, Jazwa A, Zagorska A, Dörler J, Alber H, Dichtl W, Weidinger F, Frick M, Jozkowicz A. Atorvastatin affects several angiogenic mediators in human endothelial cells. Endothelium 2005; 12: 233-241.
[23] Jan H, van Berkel TJ, Biessen EA. Induction of rapid atherogenesis by perivascular carotid collar placement in apolipoprotein E-deficient and low-density lipoprotein receptor-deficient mice. Circulation 2001; 103: 1164-1170.
[24] Lieto E, Ferraraccio F, Orditura M, Castellano P, Mura AL, Pinto M, Zamboli A, De Vita F, Galizia G. Expression of vascular endothelial growth

factor (VEGF) and epidermal growth factor receptor (EGFR) is an independent prognostic indicator of worse outcome in gastric cancer patients. Ann Surg Oncol 2008; 15: 69-79.
[25] Weidner N, Carroll P, Flax J, Blumenfeld W, Folkman J. Tumor angiogenesis correlates with metastasis in invasive prostate carcinoma. Am J Pathol 1993; 143: 401.
[26] Moulton KS, Heller E, Konerding MA, Flynn E, Palinski W, Folkman J. Angiogenesis inhibitors endostatin or TNP-470 reduce intimal neovascularization and plaque growth in apolipoprotein E-deficient mice. Circulation 1999; 99: 1726-1732.
[27] Semenza GL. Regulation of hypoxia-induced angiogenesis: a chaperone escorts VEGF to the dance. J Clin Invest 2001; 108: 39-40.
[28] Celletti FL, Waugh JM, Amabile PG, Brendolan A, Hilfiker PR, Dake MD. Vascular endothelial growth factor enhances atherosclerotic plaque progression. Nat Med 2001; 7: 425-429.
[29] Veerman K, Venegas-Pino D, Shi Y, Khan M, Gerstein H, Werstuck G. Hyperglycaemia is associated with impaired vasa vasorum neovascularization and accelerated atherosclerosis in apolipoprotein-E deficient mice. Atherosclerosis 2013; 227: 250-258.
[30] Baikoussis NG, Apostolakis EE, Papakonstantinou NA, Siminelakis SN, Arnaoutoglou H, Papadopoulos G, Goudevenos J, Dougenis D. The implication of vasa vasorum in surgical diseases of the aorta. Eur J Cardio-Thorac Surg 2011; 40: 412-417.
[31] Lee EW, Grant DS, Movafagh S, Zukowska Z. Impaired angiogenesis in neuropeptide Y (NPY)-Y2 receptor knockout mice. Peptides 2003; 24: 99-106.
[32] Ziche M, Morbidelli L. Nitric oxide and angiogenesis. J Neurooncol 2000; 50: 139-148.